FACULTY OF ENGINEERING AND ARCHITECTURE

Evaluating the human exposure of a UAV-aided network

Thomas Detemmerman
Student number: 01707806

Supervisors: Prof. dr. ir. Wout Joseph, Prof. dr. ir. Luc Martens
Counsellors: Dr. ir. Margot Deruyck, German Dario Castellanos Tache

Master's dissertation submitted in order to obtain the academic degree of
Master of Science in Information Engineering Technology

Academic year 2019-2020

GHENT UNIVERSITY

Dankwoord

todo

Contents

Glossary **10**

Acronyms **11**

1 Introduction **12**

1.1 Outline of the issue 12

1.2 Objective 13

1.3 Structure 13

2 State of the art **15**

2.1 Deployment tool for an UAV network 15

2.2 Electromagnetic exposure 16

2.2.1 Electromagnetic field radiation 16

2.2.2 Specific absorption rate 17

2.2.3 Related work 17

2.3 Optimizing towards electromagnetic exposure and power consumption 18

2.4 Technologies 18

2.4.1 Type of drone 18

2.4.2 LTE 19

2.4.3 Type of antenna 19

3 Scenarios **22**

3.1 A single user 22

3.2 Increasing traffic with only one drone available 23

3.3 Increasing traffic with an undifend amount of drones 24

4 Methodology **25**

4.1 Tool 25

4.2 Electromagnetic exposure 25

4.2.1 Calculation of total whole body SAR10g 25

4.2.2 Calculating downlink expsure 26

4.2.3 Uplink exposure 27

4.2.4 Defining an antenna 29

4.2.5 Radiation pattern 31

4.3 Optimizing the network 32

4.4 Implementation 34

4.4.1 Network planning 34

4.4.2 Implementation of the radiation pattern 34

4.4.3 Performance improvement 36

5 Results and discussion **38**

5.1 Number of simulations 38

5.2 Scenario 1: one user and one basestation 40

5.2.1 The influence of the fly height on SAR_{10g} 40

5.2.2 The influence from the maximum transmission power 40

5.3 Scenario 2: increased traffic 41

5.3.1 Influence of the flight altitude 41

5.4 Scenario 3: 41

6 Conclusions **43**

Appendices **46**

A Radiation patterns: datasheet **47**

B Radiation patterns: example configuration **49**

List of Figures

2.1 General design of a microstrip antenna 20

4.1 Design of the microstrip patch antenna. 31

4.2 Radiation pattern 1: 3D model of the entire pattern on the left with the configuration as discribed above. In the middel a 2D radiation pattern of the E-plane and at the right a 2D model of the H-plane. 32

4.3 Radiation pattern 2: Generated with a groundplane of 0.06m by 0.06m. On the left is the 3D model of the entire pattern plotted. In the middel a 2D radiation pattern of the E-plane and at the right a 2D model of the H-plane. 33

4.4 Schematic example of slices in a radiation pattern. 35

4.5 Schematic example of how bilinear interpollation works. 36

4.6 Example of a KD-three in two dimensions 37

5.1 General design of a microstrip antenna 39

5.2 General design of a microstrip antenna 39

5.3 General design of a microstrip antenna 39

5.4 General design of a microstrip antenna 41

5.5 General design of a microstrip antenna 42

5.6 General design of a microstrip antenna 42

List of Tables

2.1 specifications for the used drone. 19

3.1 Overview of the configuration. 23

3.2 Overview of the configuration. 23

3.3 Overview of the configuration. 24

4.1 Overview of configuration parameters 29

5.1 Overview of the configuration. 38

A.1 Overview of attenuation in dBm 48

List of Listings

1 Mathlab code to generate radiation pattern for a microstrip patch antenna . . . 32
2 Example configuraton of a radiation pattern. 50

Glossary

equivalent isotropic radiator A theoretical source of electromagnetic waves which radiates the same intesity in all directions.. 19, 20, 37

spurious radiation according to the thefreedictionary.com: Any emission from a radio transmitter at frequencies outside its frequency band. Also known as spurious emission.. 17

Acronyms

DL downlink. 15, 16, 24, 26

EIRP Equivalent Isotropical Radiation Power. 23

FDD frequency division duplex. 16

ICNIRP International Commission on Non-Ionizing Radiation Protection. 13, 14

IEC International Electrotechnical Commission. 25

LTE Long-Term Evolution. 16, 37

SAR Specific Absorption Rate. 14, 25

TDD time division duplex. 16

UABS Unmanned Arial Base Station. 10, 12, 13, 15, 19, 26, 30–34, 36, 37

UE User Equipment. 10, 13, 19, 20, 23–26

UL uplink. 14–16, 26

1

Introduction

1.1 Outline of the issue

Society is constantly getting more and more dependent on electronic communication. On any given moment in any given location, an electronic device can request to connect to the bigger wireless network. Devices need more then ever to be connected, starting from small IOT sensors up to self-driving cars which needs to be supported by the existing infrastructure.

Once again it becomes clear why we're on the eve of a new generation of cellular communication named 5G. This new technology is capable of handling millions of connections every square meter while satisfying only a few microseconds of a delay and providing connections up to 10Gbps [1].

Also in exceptional and possibly life-threatening situations, we rely on the cellular network. For example during the terrorist attacks in Zaventem, a Belgian city. Mobile network operators saw all telecommunications drastically increasing causing moments of contention. Some operators decided to temporarily exceed the exposure limits in order to handle all connections. [2]

Electromagnetic exposure can however not be neglected. Research shows how exesive electromagnetic radiation can cause diverse biological side effects [3]. Because of public concern, the World Health Organization had launched a large, multidisciplinary research effort which eventually concluded that there was no sufficient evidence that confirmed that exposure to low level

electromagnetic fields harmfull is [4]. Nevertheless remains the public very concerned about potetial health risks.

1.2 Objective

In this master dissertation the electromagnetic exposure of a user is investigated taking all prominent sources into account which include the user's own mobile device, basestations and other users their User Equipment (UE).

In order to determine the magnitude of exposure to which users in a certain area are exposed, various values need to be known. Not only the used technology but also the position of users and basestations need to be known. To make this research possible, an existing planning tool is used which gives insight in users and basestation distributions. Bitrates of idividual users, power useage of the different electronical devices and which basestations handels which users. The tool describes in other words a fully configured network. In this way, all needed parameters will be known.

The electromagnetic exposure will then be analysed by applieing the tool in different scenarios. During the simulations it is investigated how various input variables influence the network.

The calculation of electromagnic exposure originating from base stations is discussed in variously discussed in litterture. Papers who convert electromagnetic exposure into a single value is rather limited. Not only how electromagnetic exposure behaves but also related values like power consumption or even coverage.

research question 1: How can a Unmanned Arial Base Station (UABS) network be optimized to minimize global exposure and overal power consumption? What are the effects on the network?

research question 2: What are the advantages and disadvantages of a model as described in research question 1 compared the the already existing pahtloss oriented model.

research question 3: How does the UABS fly height influence uplink and downlink exposure?

1.3 Structure

TODO: update this section

The following chapter 2 exists of several succesive sections explaining how the electromagnetic exposure of a single human being is calculated. The first section 4.2.2 explains how the exposure is calculated between a user and a single femtocell. Section 4.2.2 defines how to combine all exposures from the different femtocells towards a single users. Finaly, section **??** explains how directional antenna's are taken into account.

2

State of the art

2.1 Deployment tool for an UAV network

The tool is also able to calculate a more precisly pathloss since

The calculation of electromagnetic radiation require several input values which need to be known. To fullfill this, a deployment tool developped by The WAVES research group at UGent has therefore developed a deployment tool which distributes UAVs equiped with femtocell base stations. These kind of UAVs will be called a UABS.

A deployment tool for an UAV-aided emergency network is described in [5]. The idea is that in case of a disaster, the existing network might be damaged and won't be able to handle all users who are trying to reconnect to the backbone network. A fast deployable network is suggested in [5] by using UABSs. These are UAVs equiped with femtocell base stations and will be distributed over the disaster area, orchestrated by the deployment tool.

The deployment tool will try to calculate the optimal placement for each UABS and requires therefore a description of the area where the UAV-aided network needs to be deployed. This is done with the use of so-called shape files. Theses files contains tree dimensional descriptions of the buildings present in the area and are key values in approaching results as realistic as possible. Furthermore, the tool also requires a time period and a configuration file containing

technical specifications of the type of UABS that is being used. The tool will thereafter randomly distribute users over the area and assigns a certain bitrate to them.

In a second phase, the optimal possition for each UABS is calculated. This is done by trying to locate a UABS above each active user. Two options are possible. If a flighheigt is defined, a basestations is placed above each user at the given height, unless a building is abstructing it's location. Then, no basestation will be located above that user. If no flighheigt is given to the tool, the basestation is located 4 meters above the outdoor user or 4 meters above the building where the indoor user resides. The later is only allowed if the suggested heigt remains below the given maximum allowed height.

Finally, all UABS are sorted on wether they were active or not, followed by the increasing pathloss from each UABS to that user. So the algirtm starts by checking for each active UABS if it can cover the user. If this is the case, the user will be connected to this UABS. If not, the second active basestation with a (slightly) worse pathloss is considered. If no active basestation is suitable, inactive UABS are considered. The user remains uncovered if no UABS is found. The reasoning behind first only considering basestations that are already active is the hight cost that comes allong with each drone.

Up till now, the tool has only calculated some suggestions. The effective provisioning is done in the fourth phase where drones are sorted by the ammount of users it covers. As long as UABS are available in the facility where they reside, UABS are provisioned and its users are marked as covered.

2.2 Electromagnetic exposure

2.2.1 Electromagnetic field radiation

People in a telecommunication network are exposed to far field electromagnetic radiation originating from basestations and other UE. Network planners need to make sure that the the electromangteic fields (expressed in V/m) does not exceed limitations enforced by the government. These limits are location dependend. The european union recommend the guidlines as defined by the International Commission on Non-Ionizing Radiation Protection (ICNIRP) which limits electromagnetic exposure to 61 V/m. Each european country needs to decide for themselves which limitations to enforce. Belgium for example delegated this responsibility to Flanders, Brussels and Wallonia [6].

The used deployment tool is applied in Ghent, a Flamish city in Belgium. The standards defined

by the flamish governent is therefore applicable. They state that in the 2.6 Ghz frequency band, an individual antenna can't exceed 4.5 V/m and the cummulative sum of all fixed sources 31 V/m [7].

2.2.2 Specific absorption rate

Specific Absorption Rate (SAR) represents the rate that electromagnteic energy is absorption by human tissue with the thermal effect as it's most important consequence. The ICNIRP has concluded that the threshold effect is at 4 W/kg meaning that any higher absorption rate would overwhelm thermoregulatory capacity of the human body. Whole body values between 1 and 4 W/kg increases the temparture of human body less then 1°C which is proven not to be harmfull for a healthy human being[8]. Thereafter, a safety margin is introduced to tackle unknown variables like experimental errors, increased sensitivity for certain population groups and so on. This results in a whole body SAR_{10g} of $0.8W/kg$ and $2W/kg$ for localized SAR_{10g} values for the head and torso aera [6].

2.2.3 Related work

The goals of this master dissertation is the investigation of electromagnetic exposure considering all sources. Three types of sources are considered: electromagnetic radiation caused by basestations, near field radiation from the users own device and far field radiation originating from other users their equipment. This electromagnetic radiation is thereafter absorbed by the human body which will be expressed in SAR values. Different type of SAR-values exist like whole body SAR which is the average absobed radiation over the entire body. Also more precise SAR-values exist which go under the name of localized SAR-values and only cover a part of the human body like the head.

Several papers exist calculating exposure originating from certain sources but very limited research has been done covering the whole picture. In [9] is described how electromagnetic radiation of several WiFi access points is being calculated. The authors of [10] used this knowledge to investigate electrmangetic exposure originating from basestations in a more outdoor environment. [11, 12] addresses the fact that also uplink (UL) traffic from the user's device should be considered. They therefore investigated indoor exposure. They did not only consider the electromagnetic radiation but also how much is absorbed by the body wich will be expressed as specific absorption rate. Since the authors only covered voice calls, uplink SAR was expressed in localized SAR values while the downlink traffic is expressed in whole body SAR. With the advent of 5G, a paper [13] has been published describing how localized SAR values are achieved from all sources. More precisly: all mobile phones and all basestations in the network after which

they converted the electromagnetic exposure to localized SAR values. Finally, [14] describes how both UL and downlink (DL) traffic can be converted in whole body SAR values making it possible to achieve an overall picture. They applied this formula howevery only for the user's own device.

In a realistic network like the used deployment tool, some users are calling while annother part is using other type of telecommunication services like browsing the web. Therefore, all absorbed electromagnetic exposure should be expressend in whole body SAR while still covering all sources.

2.3 Optimizing towards electromagnetic exposure and power consumption

UABSs are drones with femtocell base stations attached to it. Drones can remain in the air for only a limited time, which is certainly the case when also an antenna needs to be connected to the battery of the its carrier. It is therefore interessting to not only considering electromagnetic exposure of the user but also the power consumption that comes with it. However an increasing transmission powers of an antenna comes with an increasing electromagnetic exposure, this is not the case considering both values for an entire network. In fact, the autors from [10] prove that both become inversely equivelent.

If a network is optimized towards power consumption, less drones be provisioned radiating at higher power levels. This is because not only the transmission power is considered but also the power needed to keep the drone in the air. Therefore, it is cheaper to cover a user by increasing the antennas transmission power of an already activated drone nearby and prevents therefore prevets the power cost of a new drone. By increasing the transmission power, also the electomagnetic exposure will increase for users closer to that drone. An exposure optimized network will therefore faster decide to power up a new drone.

todo: geen grid maar per user

2.4 Technologies

2.4.1 Type of drone

Section 2.1 describes how femtocell antennae will be connected to helicopter drones. Two types of drones are considered in [5]: an off-the-shelf drone affordable by the generic public and a

more expensive drone. The results in [5] show that the second type will require less drones to cover the same number of users and will last longer in the air. The research in this paper will therefore be done with the usage of the second type. A technical overview of this drone is given in table 2.1.

parameter	value
Carrier power	13.0 A
average carrier speed	12.0 m/s
Average carrier power usage	17.33 Ah
Carrier battery voltage	22.2 V

Table 2.1: specifications for the used drone.

2.4.2 LTE

The tool make usage of Long-Term Evolution (LTE) which is by the general public better known as 4G which allowes better UL and DL dataspeeds compared to its predecessors and is based on an all IP architecture. LTE can cover macrocells supporting cell sizes ranging from 5 km up to 100 km. These type of antennas are usally attached to transmission towers along highways or on top of buildings. LTE supports however also smaller cells like femtocells covering only a few hunderd meters. They are therefore more portable, require less energy and won't require a telecommunication operator because of it's simplicity. Femtocell basestations are therefore used by the deployment tool. Futher, LTE also support both frequency division duplex (FDD) and time division duplex (TDD).

FDD makes simultanious UL and DL traffic possible by assiging different frequencies within the frequency range to both data streams. A small guardband is used between UL and DL directions in other to prevent interference.

TDD allowes UL and DL by splitting the time domain. Meaning that both traffic directions use the same frequency and therefore alternatly (in time) use the frequency spectrum. Again, a small time intervall is used to prevent interference in case of a slightly bad timed syncronization.

This master dissertation will make usage of FDD.

2.4.3 Type of antenna

An important part of this master dissertation is the type of antennas that will be used by the basestations. Since the deployment tool make usage of drones in other to possition the femtocell

basestations in the right posistion, conventional sector antennas as used by terestrial transmission towers won't be a good idea. The characteristics of microstrip antennas will therefore be investigaged.

Microtstrip anntenas provide several advantages compared to traditional antennas [15, 16]. Microstrip antennas are lightweight, low in cost and thin causing them to be more aerodynamic which is a usefull feature since the atennas will be attached to flying drones.

A basic microstrip antenna like figure 2.1 consisting a ground plane and a radiating patch which are seperated with a dielectric substrate. Several constructions exist like microstrip patch antenna, microstrip slot antenna and printed dipole antenna which has all similar characteristics. They are all thin, support dual frequency operation and they all have the dissadvatage of spurious radiation.The microstrip patch and slot antenna support both linear and circular polarization while the printed dipole only support linear polarization. Further is the fabrication of a microstrip patch antenna considered to be the easiest of its competitors.

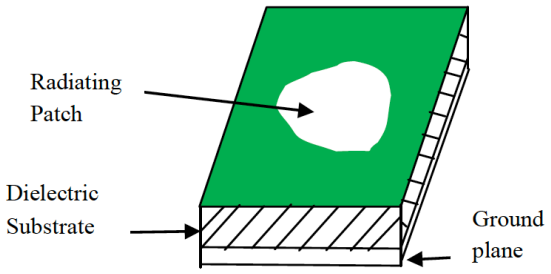

Figure 2.1: General design of a microstrip antenna

The microstrip antenna requires besides the groundplane, dielectric substrate and the radiation pach also a feed line. Several feeding techiques exists of which the most popular are: coaxial probe feeding, microstrip line and apeture coupling. (todo: more refs? gebruik nummer twee van J13 (p2))

A first feeding method is with the usage of a coaxial cable where the outer conductor is attached to the ground plane and the inner conductor to the radiationg patch. Modelling is however difficult, escpecially for thic substrates as will be used in this master dissertation. A second option is the usage of a microstrip line. This type of feeding is much easier to model since the microstrip line can be seen as en extenstion of the radiating patch. A dissadvatage is that the antenna will transmit at frequencies outside the aimed band which is also known as spurious radiation which therefore limits bandwith. A thirt is proximity coupling which has the largest bandwidth and low spurious radiation. It consist however of two dielectric substrates causing the overall thickness of the antenna to increase as well as it's fabrication difficulty. (todo: tekst te weinig, bespreek ook apperture coupled attenna (zelfde paper als de rest)) The

increasing usage of the microstrip patch antennas can be explained by it's easy fabrication and lightweightness and therefore knows a widespread application in the millitary, global possitioning systems, telemedicine and WiMax applications and so on. The authors also state that some of the dissadvatages like lower gain and power handling can be solved with the usage of an array configuration.

At last, also the materials of the antenna need to be considered. The radiationg patch mainly rectengular. In fact is any given shape possible but other configurations then a cirle or a rectangle will require large nummerical computation [16]. The radiating patch is usualy made of a thin layer of either gold or copper [16, 17]. Further is also the dielectric constant of the substrate important which typially varies between 2.2 and 12. Finding a good dielectric depends how the antenna will be deployed and it's usage. According to [17] will a lower dielectric constant with a thic substrate result in better performance, better efficiency and larger bandwiths. On the other hand will according to [16] a larger dielectric constant reduce de dimensions of the antenna which is also usefull when attaching the antenna to a limited surface. Therefore is opted for a glass as dielectric substrate with a constant of 4.4.

3

Scenarios

3.1 A single user

A first scenario will investigate how SAR_{10g} is influenced in an isolated environment meaning there is nor influence from other base stations nor other UE. The tool will provision one single drone and position it directly above the user. These results will however depend on the position of the user. If the randomly generated location of the user is indoor, the expected height of the user is half of the height of the building. Investigating the electromagnetic exposure and the drone power consumption depends however on the distance between both user and UABS. For a more consistent result, the user will therefore be positioned outside when systematically increasing the fly height. Another considered variable is the transmitting power of the UABS.

This scenario deducted with two type of antennas. First, an equivalent isotropic radiator will be used and thereafter a realistic antenna. It is expected that after the introduction of an realistic antenna, the user coverage will decrease.

The tool will therefore run different simmulations. The first group is with an equivalent isotropic radiator. A first set of simmulations is with a fixed flyheight of 100m which is the proposed flyheight by [5] but with a variable transmit power of the base station. The set investigates the influence of a variable flyheight with a constant maximum transmit power of 33dBm as defined

in [5].

Both series will also be investigated with a realistic radiation pattern. The user coverage will be compared.

The user gets a fixed possition. The exact location doesn't matter as long as it is outside. Doing so will force the UE to always be at the same height of 1.5 meters. The conclusions will be based SAR_{10g}, power consumption and transmission power. These output values depend on fly height and type of antenna. An overview can be found in table 3.1

TODO: antenna orientation

x possition user	3.7331139698609683
y possition user	51.05992485238353
height of the UE	1.5m
frequency	2600Hz

Input variables	Output variables
type of antenna	SAR_{10g}
fly height	power consumption
	transmission power

Table 3.1: Overview of the configuration.

3.2 Increasing traffic with only one drone available

The previous scenario will be extended for an increasing amount of users.

todo	todo
todo	todo
todo	todo
frequency	2600Hz

Input variables	Output variables
type of antenna	SAR_{10g}
fly height	power consumption
number of users	user coverage

Table 3.2: Overview of the configuration.

The SAR_{10g}, power consumption and user coverage will be investigated for an increasing amount of users ranging from 50 to 650 in steps of 50. The only available drone will be positioned at the fly height of 100 m as recommended in [5]. For the second case, the same output variables are investigated for a varying fly height but with a fixed number of 224 users. This case will be applied in the city center of Ghent, assuming it is an average day at 5 p.m. which means it is rush hour resulting in the highest number of simmulatanious users for the day[5]. Both cases will be investigated for the two types of antennae: the fictional equivalent isotropic radiator and the microstrip patch antenna.

3.3 Increasing traffic with an undifend amount of drones

todo	todo
todo	todo
todo	todo
frequency	2600Hz

Input variables	Output variables
type of antenna	SAR_{10g}
fly height	power consumption
number of users	number of drones

Table 3.3: Overview of the configuration.

When more drones are available, an optimization strategy can be applied. The tool checks the capacity of the basestations and decides thereafter wich basestation the user should be connected to. The original algorithm checks all pahts between the user that need to be connected with all drones. Thereafter, the drones which path experience the least pathloss and still has the capacity to cover an addition user will be selected. The authors from [10] proposed however annother optimization strategy which tries to minimize electromagnetic exposure and power consumption.

The input variables flyheight, transmit power and number of users will be used to see how electromagnetic exposure, power consumption en number of drones are influenced for different optimization strategies and type of antennas.

Since there is no fixed budget limitation, the number of drones are unlimited. The tool will therefore try to connect each user and coverage will be expressed in number of drones required to cover as much users as possible instead of having a limited number of drones as in scenario and therefore has only a limited coverage expressed in percentage.

4

Methodology

4.1 Tool

The goals

4.2 Electromagnetic exposure

4.2.1 Calculation of total whole body SAR10g

The overall SAR_{10g}^{head} can be calculated by a simple sum of individual SAR values [13]. The position of the phone is however unknown. This is because the tool assigns a bitrate to a user depending on the service he is using meaning that users in the network are not only calling but are able of browsing the web aswell. Since calculating the SAR_{10g}^{head} would imply the phone is being hold next to the head, this would result in incorrect conclusions. The induced electromagnetic radiation will therefore be expressed in function of the entire body.

$$SAR_{10g}^{wb,total} = SAR_{10g}^{wb,ul} + SAR_{10g}^{wb,dl} + SAR_{10g}^{wb,neighbours} \tag{4.1}$$

The first parameter, $SAR_{10g}^{wb,ul}$, will indicate the absorbed electromagnetic radiation in the whole body originating from the users own phone whereas the second parameter $SAR_{10g}^{wb,dl}$ will represent the absorbed electromagnetic radiation by all the basestations in the considered area. As last, $SAR_{10g}^{wb,neighbours}$ specifies the same as the previous but with electromagnetic radiation originating from other users their UE.

4.2.2 Calculating downlink expsure

Calculating exposure towards a single femtocell

To determine the total exposure of a single human being or even of the entire network, the electric-field $\vec{E}$ of a single femtocell i should be calculated. The formula to determine this electromagnetic value E (expressed in V/m) for a specific location is given in equation 4.2.

$$E_i = 10^{\frac{EIRP - 43.15 + 20*\log(f) - PL}{20}} \tag{4.2}$$

TODO: write EIRP - Attenuation (A t)
This formula requires several values to be known. The frequency f on which the tranmitting antenna is operating is expressed in MHz. The other values are explained in 4.2.2 and 4.2.2.

Equivalent Isotropical Radiation Power A directional antenna can achieve gain by focussing it's input power into certain directions. By doing this, some areas experience a decreased radiation power in order to gain radiation power in the other privileged areas. If a theorical isotropic radiator todo: uileggen wat isotropic radiator isexisted, the Equivalent Isotropical Radiation Power (EIRP) is the power it would require to achieve the same power level as the actual antenna's main lob. The main lob is the area of the directional antenna experiencing the most gain. This EIRP value can be calulated as described in eq 4.3.

$$EIRP = P_t + G_t - L_t \tag{4.3}$$

Pathloss At last, formula 4.3 requires the path loss (dB). In order calculate the path loss, an appropiate propagation model is required. Several propagation models exists and the tool already uses the Walfish-Ikegami model [5]. This is because the Walfish-Ikegami model performs well for femtocell networks in urban areas. The chosen propagation model consists of two formulas depending on whether a free line of sight between the user and the basestation exist or not. Both formulas expect a distance in kilometer.

input power hangt af van bs tot bs.

Attenuation todo

Combining exposure

Since the user location in the UAV-aided network is known, the exposure is not calculated for gridpoints but for active users. compared to gridpoints in ref state of art manets -> exosure combineren

$$E_{tot} = \sqrt{\sum_{i=1}^{n} E_i^2} \tag{4.4}$$

Converting downlink electromagnetic exposure to SAR_{10g}^{wb}

Formula 4.1 expects that the DL electromagnetic radiation is converted into $SAR_{10g}^{wb,dl}$. The conversion constant is based on Duke from the Virtual Family. Duke is a 34-year old with a weight of 72 kg, an height of 1.74 m and body mass index of 23.1 kg/m [14]. This conversion factor $SAR_W^{DL}Bref$ for WiFi is $0.0028\frac{W/kg}{W/m^2}$. Since WiFi at a frequency of 2400 Mhz is very close to LTE at 2600 Mhz, it is assumed in **??** that these values are also applicable for LTE.

$SAR_W^{DL}Bref$ are expressed in power flux density S (with units $\frac{W/kg}{W/m^2}$). The DL exposure from 4.2.1 are expressed in V/m and should therefore first be converted.

$$S = \frac{E^2}{337}$$

$$SAR_{10g}^{wb,dl} = S * 0.0028$$

4.2.3 Uplink exposure

specific absorption rate into the head

todo: de 10g slaat al op localized, vandaar dat het maar 10g is, anders is het whole-body todo: we kunnen niet sar10gmax gebruiken want This means that the SAR calculations will be worst-case and possibly an overestimation of the real localised SAR. (herwoorden voor plagiaat)

Human exposure caused by downlink traffic is a not negligible asset. However, telecommunications is not a one-way street. When connecting to a UMTS network, also uplink data caused by the UE should be considered. UE generates, just like femtocells, electromagnetic waves to which a user is exposed. A part of this radiation goes to the femtocell, another part enters the body of

its user. How much electormagnic strenghts enters the body is defined as SAR and is measured with 10g biological tissue which represents the human skin. This value will from now on be expressed as SAR_{10g}. A mobile device induces two types of exposure: local and whole-body. Whole-body exposure can be neglected compared to the much higher local exposure[?]. From now on, SAR_{10g} implicitly means local exposure. International Electrotechnical Commission (IEC) defines in IEC:62209-2 a maximum for a 10g tissue SAR_{10g}^{max} as 2 W/kg and a maximum for a 1g tissue SAR_{1g}^{max} as 1.6 W/kg. Most countries, including Belgium, enforce the 10g model and will, therefore, be the point of reference for this master dissertation. The SAR_{10g} values are phone dependent. The reported values by companies of mobile devices are worst-case scenarios meaning that the values are measured when the phone is transmitting at maximum power. This is an understandable decision but won't result in a realistic scenario since modern cellular networks use power control mechanisms to prevent over radiation of a nearby device. UE will therefore never use more energy than necessary to maintain a connection. To compensate for this overestimation, the actual SAR_{10g} of each user will be predicted. These will, however, remain an estimation since the position of the phone related too the head differs from user to user. For example, by holding the phone differently, a hand can absorb more or less electromagnetic radiation. TODO: bron.

$$SAR_{10g} = \frac{P_{tx}}{P_{tx}^{max}} * SAR_{10g}^{max} \tag{4.5}$$

Equation 4.5 is used to predict the actual SAR_{10g} of a certain user. The SAR value is different for each mobile device. An average is calculated based on 3516 different phones from various brands using an up-to-date German database [18]. When the phone is positioned at the ear, an average of 0.7 W/kg is found with a standard deviation of 0.25 W/kg which are very similar results as in Ref. [?]. The median of 0.67 is used.

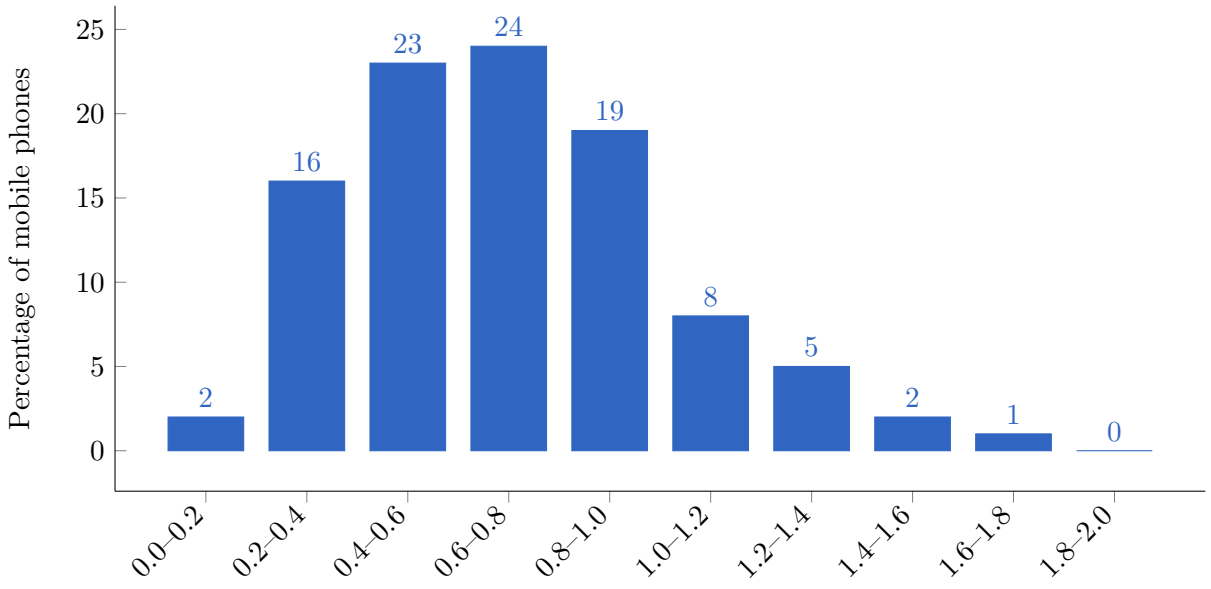

todo: xlabel, zeggen dat bovengrens niet inbegrepen is en titel geven.

The P_{Tx}^{max} is for LTE and UMTS 23 Dbm [19, 11].

To predict the effective transmitted power by the UE, the folowing equation is used:

$$P_{Tx} = P_{sens} + PL \tag{4.6}$$

Converting uplink electromagnetic exposure to SAR_{10g}^{wb}

Just like the DL radiation expects formula 4.1 the UL radiation to be expressed as SAR_{10g}^{wb}. Therefore, the conversion factor from [14] for WiFi is reused as explained in 4.2.2.

$$SAR_{10g}^{wb,ul}\left(\frac{W}{kg}\right) = 0.0070\left(\frac{W/kg}{W}\right) * P_{tx}(W) \tag{4.7}$$

4.2.4 Defining an antenna

A microstrip patch antenna is chosen because it allowes easy production but more important it has a low weight and has a thin profile causing it to be very aerodynamic which is usefull when attaching it to an UABS [20].

The dimensions of the antenna depend on the frequency it is operating and the characteristics of the used substrate. The antennas will be radiationg at a center frequency f_0 of 2.6Ghz. A substrate with a higher dielectric constant and low height reduces the dimentions of the antenna and a lower dielectric constant with a high height improves antenna performance. The used substrate will therefore be glass with a dielectric constant of 4.4. The height of the antenna is also limited to 2.87 mm in order to keep the antenna light and compact [16]. The formulas from [16] are [17] applied.

description	symbol	value
center frequency	f_0	2600 Hz
dielectric constant	ϵ_r	4.4
heigt of the substrate	h	0.00287m

Table 4.1: Overview of configuration parameters

$$W = \frac{c}{2 * f * \sqrt{\frac{\epsilon_r+1}{2}}} \tag{4.8}$$

Which C the speed of light, f being the center frequency of 2600 Hz and a dielectric contanst of $\epsilon_r = 4.4$ a width of 3.51 mm is achieved.

$$\epsilon_{reff} = \frac{\epsilon_r + 1}{2} + \frac{\epsilon_r - 1}{2} * \left(1 + 12 * \frac{h}{W}\right)^{-\frac{1}{2}}$$

The height of the dielectric is choses to be 2.87mm in order to keep the antenna smal and light**??**. ϵ_r is the permitivity constant of the substrate and depends of the used matieral. In this paper, a substrate like glass is chosen because of the high dielectric constant of $\epsilon_r = 4.4$ compared to other matierals like teflon with only a dielectric constant of $\epsilon_r = 2.2$ This is because larger dielectric decreases the dimentions of the antenna patch **??** and therefore indirectly also decreases the dimentions of the entire antenna surface which comes in handy for the limited space on drones. When substituting these values, a ϵ_{reff} of 3.91 is determined.

$$L_{eff} = \frac{c}{2 * f * \sqrt{\epsilon_{reff}}} \tag{4.9}$$

Applying this formula with the known values of above the L_{eff} results in 29.16 mm.

$$\Delta L = 0.412 * h * \frac{(\epsilon_{reff} + 0.3)\left(\frac{W}{h} + 0.264\right)}{(\epsilon_{reff} - 0.258)\left(\frac{W}{h} + 0.8\right)} \tag{4.10}$$

By substituting the values from above, the length extension determines that ΔL equals 1.3071 mm.

Finally can the lenght of the patch be calculated using the expression: $L = L_{eff} - 2 * \Delta L$ which result in 26.55 mm which result in an antenna like 4.1.

The transmission line model is in fact only applicable for an infinite ground plane but it has been proven that similar results can be achieved if the groundplane's dimentions are bigger then the patch of approximatly 6 times the height of the dielectric substrate [16, 17].

$$L_g = 6 * h + L \tag{4.11}$$

$$W_g = 6 * h + W \tag{4.12}$$

Therefore should the lengt of the groundplane L_g be at least 0.0438m and a width of W_g 0.0524m.

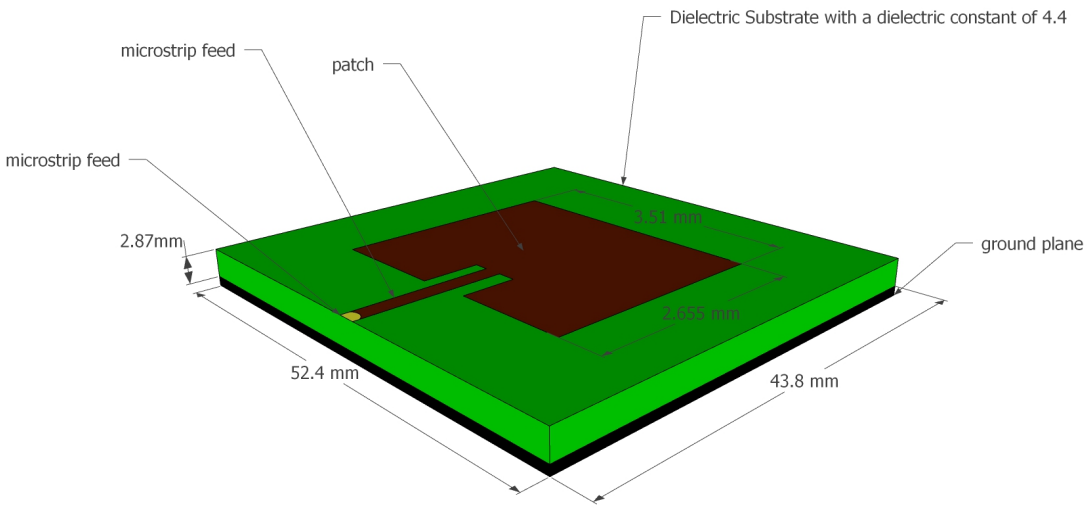

Figure 4.1: Design of the microstrip patch antenna.

4.2.5 Radiation pattern

Mathlab is able to generate the radiation pattern for the this microstrip patch antenna. The code in 1 starts with defining the dielectric substrate which will be glass with a dielectric constant of 4.4 and a height of 0.00287m. Thereofter is de microstrip patch antenna generated with the width and lenght being the dimensions of the radiation patch and the GroundPlaneLength and GroundPlaneLength the dimensions of the groundplane and dielectric substrate. The FeedOffset is the releative offset from the center where the radio frequency power is fed to the radiating patch which here wil be at the edge which is in figure 4.1 is indicated with the yellow dot. At last is the dielectric object given to the patchMicrostripInsetfed object.

Generating the pattern is done with the 'pattern' command. The first value is the patchMicrostripInsetfed object followed by the frequency in wich the antenna will be operating. Optionaly can a azimuth value be parsed like in line 7 and 8 where 90 and 0 stand for relatively the H-plane and E-plane.

Running the configuration from 1 will generate the radiation pattern from figure 4.2. When running the same configuration for a slitly bigger square antenna with an edge of 0.060m, the radiation pattern from 4.3 is achieved. It becomes clear that the radiation pattern from figure 4.2 has a higher attenuation in de direction it is not facing compared to the radiation pattern of figure figure 4.3. If it is assumed that drones fly lower then users are possitioned in some buildings, the pattern of 4.2 would be a better approach. However, for the continuation in this master dissertation, the radiation pattern from figure 4.2 is assumed since the antenna is the

```
d = dielectric("Name",'glass',"Thickness",0.00287,"EpsilonR",4.4)
p = patchMicrostripInsetfed("Width",0.0351,"Length",0.02655,
    "GroundPlaneLength",0.0438,"GroundPlaneLength",0.0524,
    "FeedOffset",[-0.021885 0],"Substrate", d)

pattern(p,2.6e9, "CoordinateSystem", 'polar', "Normalize",true)
pattern(p,2.6e9, 90, "CoordinateSystem", 'polar', "Normalize",true)
pattern(p,2.6e9, 0, "CoordinateSystem", 'polar', "Normalize",true)
```

Listing 1: Mathlab code to generate radiation pattern for a microstrip patch antenna

smallest and therefore more suitable to attach to the limited space available under the drone. A datasheet of the exact values from both radiation patterns can be found in appendix A.

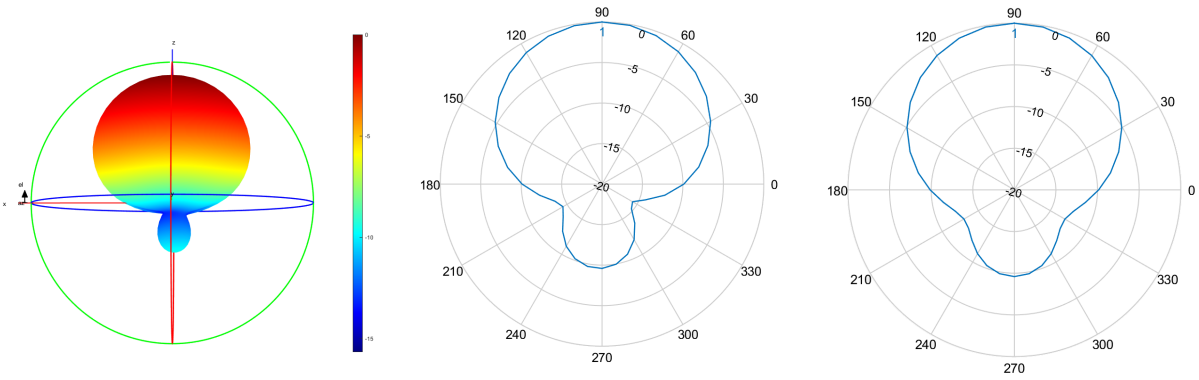

Figure 4.2: Radiation pattern 1: 3D model of the entire pattern on the left with the configuration as discribed above. In the middel a 2D radiation pattern of the E-plane and at the right a 2D model of the H-plane.

4.3 Optimizing the network

The network as originally defined in the deployment tool tried to minimize power consumption by connecting the user to a basestations which experienced the lowest path loss. A second optimization strategy is introduced, based on the fitness function described in [10].

$$f = w * \left(1 - \frac{E_m}{E_{max}}\right) + (1 - w) * \left(1 - \frac{P}{P_{max}}\right) * 100 \tag{4.13}$$

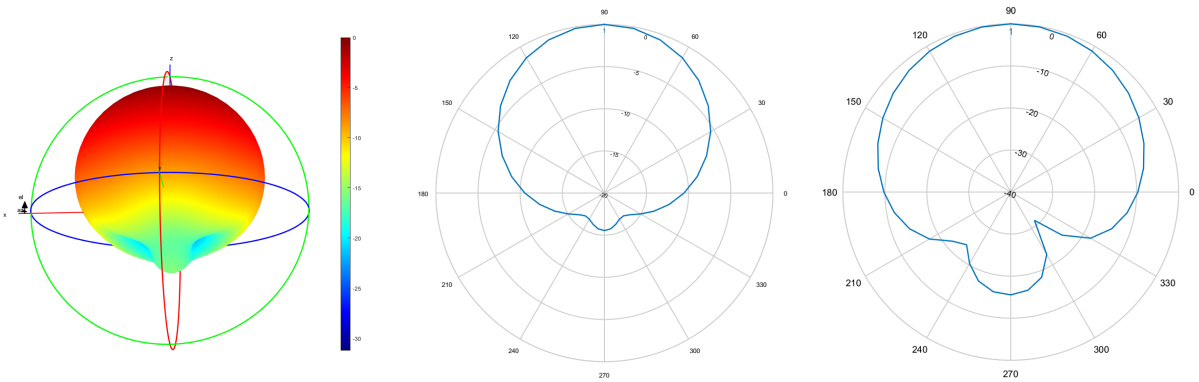

Figure 4.3: Radiation pattern 2: Generated with a groundplane of 0.06m by 0.06m. On the left is the 3D model of the entire pattern plotted. In the middel a 2D radiation pattern of the E-plane and at the right a 2D model of the H-plane.

Forumla 4.13 retuns a fitness value. Users are connected to different UABSs and each time the fitness value is calculated. The user will eventually be connected to the drone which resulted in the highest fitness value. This process is repeated for each user. w is the importance factor of electromagnetic exposure ranging from 0 to 1 with boundaries included. A w set to zero means that electromagnetic exposure is not important and therefore be called an power consumption optimized network. Likewise, a w set to one will be called an exposure optimized network. P_max is the power consumption if all UABSs are active and would be radiating at the highest possible level and P the used power by the current network. This will be the power required for the flying drones themselves and there antenae. E_m will be the exposure for the current designed network and E_{max} the electromagnetic exposure when all antenae are at their highest power level.

The weighted average E_m can be found by inserting the median and 95 percentile from all exposures into formula 4.14. Since the location of all users in the deployment tool are known, it is sufficient to calculate exposure only in those possitions.

$$E_m = \frac{w_1 * E_{50} + w_2 * E_{95}}{w_1 + w_2} \tag{4.14}$$

w_1 and w_2 in 4.14 being the weighting factors. Not only the median exposure is important but also limiting higher exposure is important. Just like [10] is with that reason w_1 and w_2 chosen to both have an equal importance of 50 %. todo: in J1 is dit gedetailleerder uitgeschreven. Mogelijk om hier wat extra over te schrijven.

4.4 Implementation

4.4.1 Network planning

TODO Thereafter, all inactive users are deleted and only the x best bs are kept with x equal to facilityCapacity. Eventually, exposure is one last time calulcated and objects are initilized with the correct exposure values.

4.4.2 Implementation of the radiation pattern

The deployment tool originally only supported EIRP antennas. The tool thus has been exteded and is fully configurable allowing any possible antenna in any possible orientation using the XML-file describing the femtocell. The configuration descripted in this file applies to all UABSs.

The orientation is done using two values called 'downtilt' and 'north offset'. The first value defines the downtilt angle under wich the antenna is pointing. An angle of 0 degrees is perfectly horizontal and pointing straight to the ground is done with an angle of 90°. This parameter only supports postive values ranging from zero to 360 (upper boundary not included). An antenna pointing to the sky would therefore require a value of 270°. The second value, the north offset, difines the azimuth orientation of the drone. The value given to this parameter indicates the offset between the north and the horizontal direction the antenna should be pointing. The value should once again range from 0° to 360° with the upper boundary not included. The angle is calculated in counter clock wise orientation. For instance, a north offset of 270° will let the UABS point to the east.

Thereafter, the normalized radiation pattern is supplied to the tool. The actual pattern is three dimensional. To simplefy this, slices perpendicular to the az-axis are extracted. These are indicated at figure 4.4 with azimuth cut. whith an angle of of 90°, four slices are achieved, easch consisting out of elevation cuts. The intersection of an elevation and azimuth plane corresponds with a certain attenuation which is fed to the tool. Figure 4.4 show only 3 elevation planes. The radiation pattern used in the tool has an attenuation every 10°. In other words, a slice consist of 19 values raning from 0° to 180° (boundaries included).

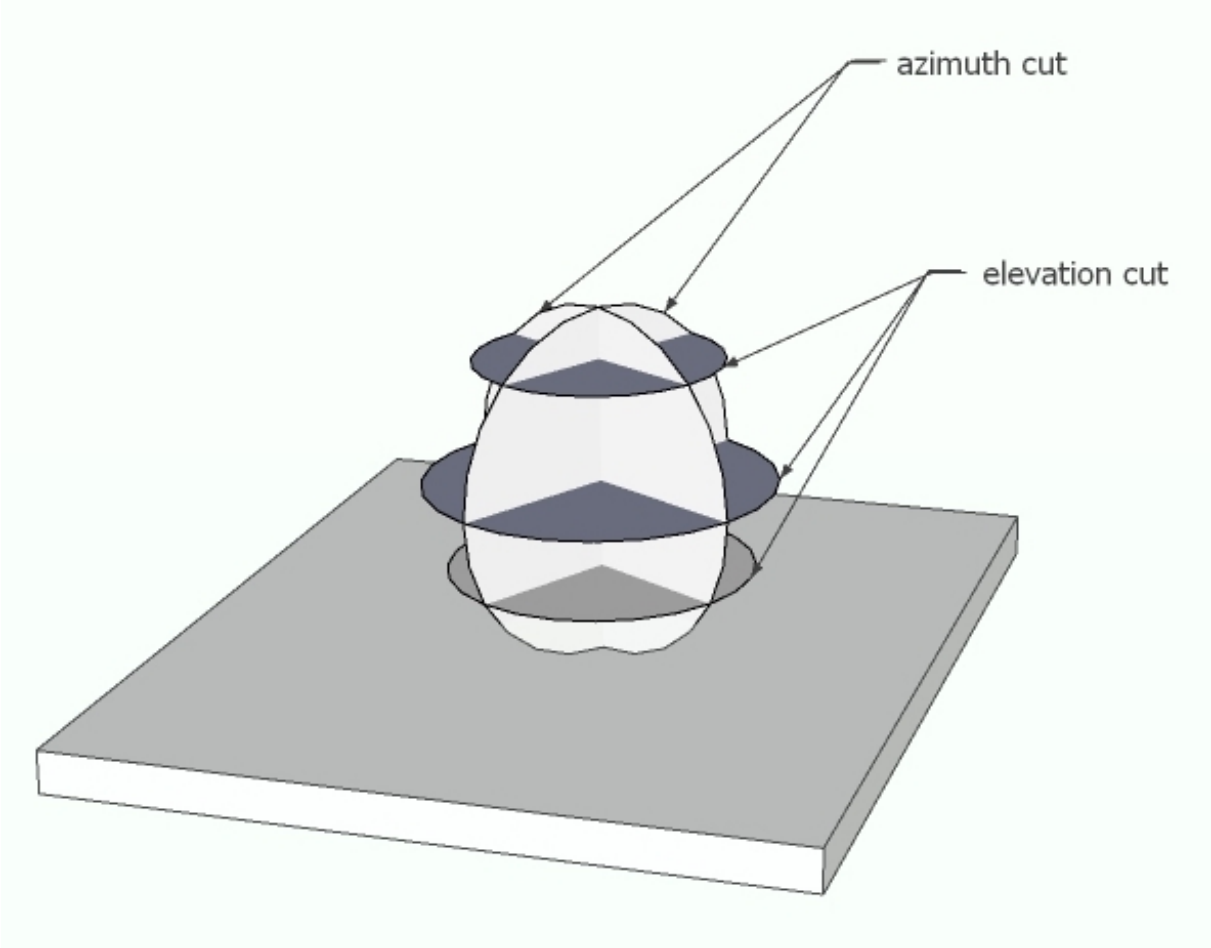

Figure 4.4: Schematic example of slices in a radiation pattern.

The number of required sliced depend on the complexity of the radiation pattern. For symetrical radiation patterns like in figure 4.2 and 4.3, two cuts perpendicular to each other deviding the radiation pattern in 4 slices is defently sufficient. However, this might not be sufficient for radiation patterns with a more complex structure containg several side lobs. To tackle this issue, as mutch azimuth-slices as desired can be defined. Each slice should however contain an equal ammount of elevation slices. A concrete example can be found in appendix X

When the attenuation of a certain user to that UABS needs to be calculated, the angle needs to be calculated TODO: schrijf hierover.

The change is very little that the angle for which the attenation is requested is known. The attenuation should therefore be esitmated using bilinear interpollation.

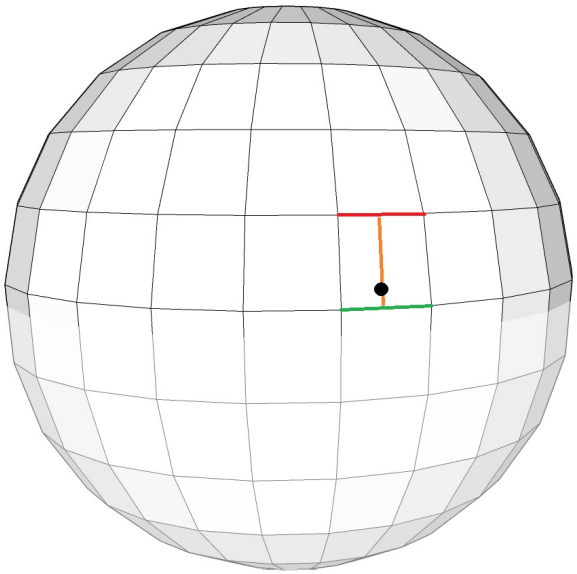

Figure 4.5: Schematic example of how bilinear interpollation works.

4.4.3 Performance improvement

Calculating pathloss

The pathloss is required for several formulas. For instance, each user decides whether a UABS is feasable based the pathloss but also the calculations for the downlink electromagnetic exposure require this value to be known. The formulas for the whole body SAR_{10g} require not only the pathloss between the user and all UABSs but even the pathloss between users themselves. These pathloss calculations are based and the Walfisch-Ikegami Model and makes a distiction between line-of-sight and non-line-of-sight situations causing a high computational load. The caculation between two points stands completly free from any other calculation between any other point and is therefore a suitable candidate to be multithreaded. The deployment tool creates two thread pools. The first pool creates a thread for each user where each thread calculates the pathloss between the user assigned to him and all possible UABSs causing a time complexity of n^2. Each user stores all pathlosses between himself and any other UABS and result therefore in a total space complexity of n^2. When all users are finished, the pool is shut down and a second one is created for the same calculations but between users. The pool will, just like the previous, create threads for each user but has an important difference. When a certain user calculates the pathloss to another user, this pathloss also applies for the other direction. The tool saves time by calculating the pathloss only once and stores the pathloss with both users. It is therefore sufficient that a given user only calculates pathlosses to users left of him, since the other will

be calculated by the users right to him. This results in a time complexity of only $n(\frac{n}{2})$. When the last user finishes his thread, all users know the pathloss to all other users causing a space complexity of $n(n-1)$.

Limiting antenna searching

The user needs to be connected to the 'best' basestation. To indentify this best UABS, the user should be connected to each basestation and the fitness value 4.13 of the network should be evaluated. The connection which resulted in the best fitness function will be added in the solution. This process is repeaded for each user but can further be improved. A user will likly be connected to either UABS directly above him or to a UABS in the direct neighbourhood. Time complexity can thus be improved by not considering drones outside a certain radius. An ideal datastructure for neighbourhood-search is a KD-tree. This datastructure is based on a binary tree and optimal for objects with multiple keys. Objects are thus positioned in K dimensions, each node split the hyperplane over exact one dimension. The dimension that need to be splitted depends on the level of the KD-tree where that node is situated. In this case, the x and y coordinate will be used in a 2D-tree (k=2) like in figure 4.6.

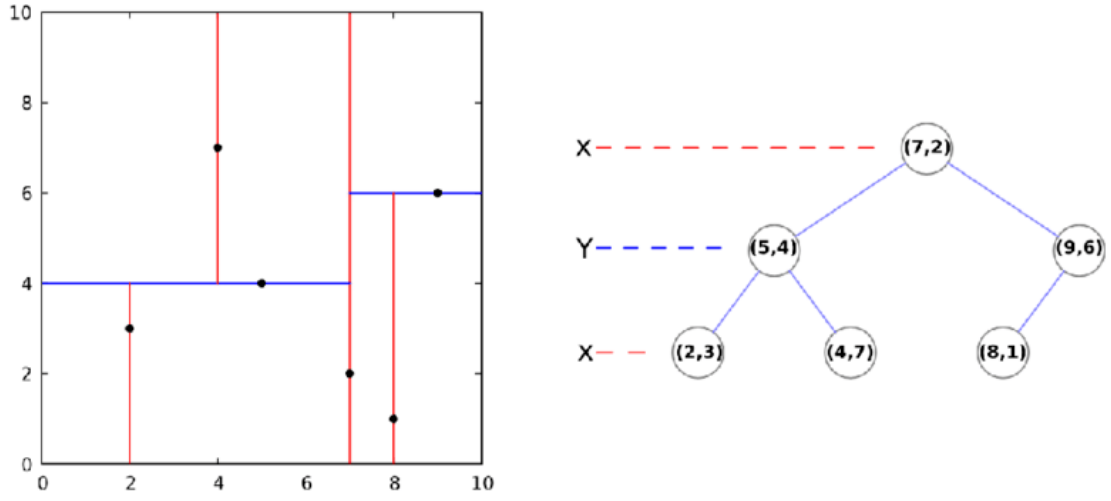

Figure 4.6: Example of a KD-three in two dimensions

Here, is chosen to consider only UABSs whithin a radius of half a kilometer. In a scenario of 500 UABSs, 60 possible UABSs are verified. TODO: schrijf ook voor 200 users.

5

Results and discussion

5.1 Number of simulations

The algorithm makes usage of randomly distributed users causing each simulation to be difference. The results are based on average values over multiple simulations. It is therefore important knowing how mush simulations is required in order to become a converged average. This is done by using an example scenario which details can be found in table **??**. The most important parameters investigated in the different scenarios are SAR_{10g}, power consumption and user coverage. Therefore, the cummulative avarage of each investigated value is plotted in function of number of simulations.

Parameter	value
number of users	40
facilityCapacity	20
fixedFlyHeight	100
optimization strategy	power consumption optimized

Table 5.1: Overview of the configuration.

The number of simulations has a direct influence on the runtime. Certain configurations take a considerable amount of runtime (expessed in hours). This is because of the exponential time

complexity. The deployment tool with n users, will need to calculate n times the pathloss between n drones and n users and thereafter $n/2$ times between each user. Thereafter, each user will have to be connected to the best possible UABS and each user is therefore required to consider multiple UABSs.

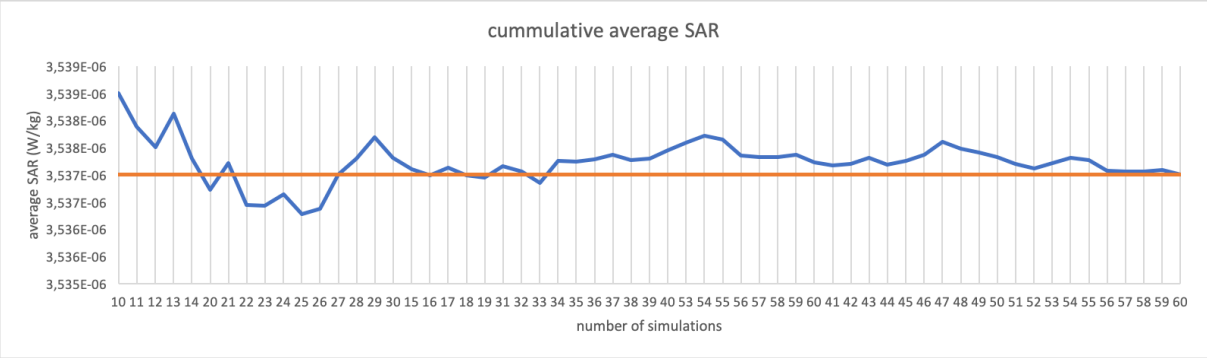

Figure 5.1: General design of a microstrip antenna

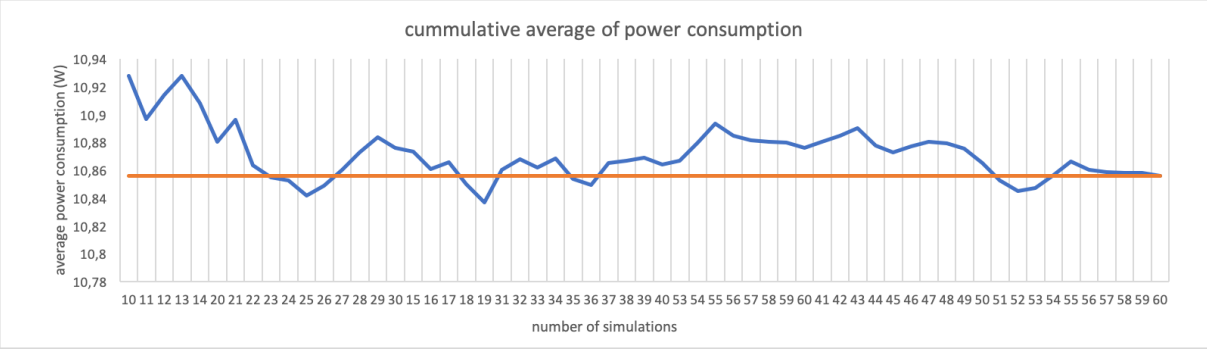

Figure 5.2: General design of a microstrip antenna

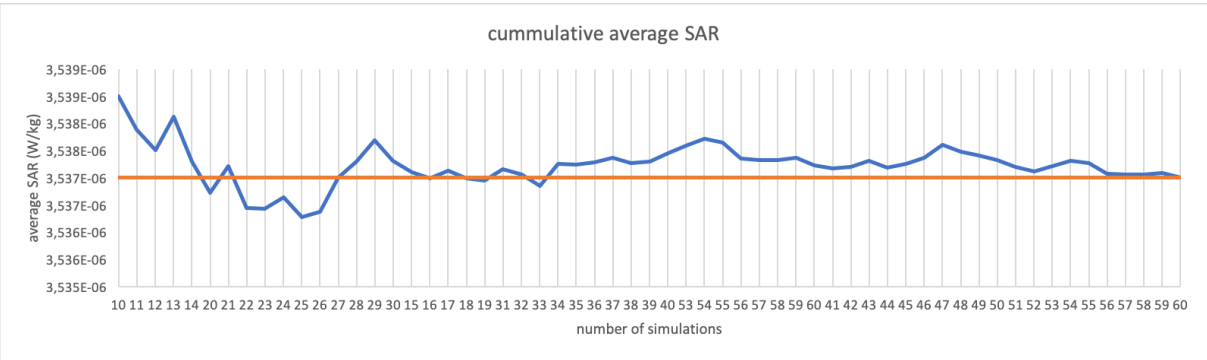

Figure 5.3: General design of a microstrip antenna

5.2 Scenario 1: one user and one basestation

5.2.1 The influence of the fly height on SAR_{10g}

This section investigates how the fly height of the UABS influence SAR_{10g} and power consumption. In figure 5.4 becomes clear that with an increasing flyheight, the specific absorption rate grows exponentially which is also the case for the power consumption (fig. 5.5)

This behavior has been examined for the two types of antennae which are the fictional equivalent isotropic radiator and the microstrip patch antenna. In figures 5.4 and 5.5 becomes clear that the type of antenna does not influence the power consumption nor the specific absorption rate in this scenario. The reasoning behind this is that the tool will possition the UABS just above the user. An equivalent isotropic radiator doesn't experience attenuation while a microstrip patch antenna does. The later is however pointing to the ground meaning the user is in the perfect center of the main beam and therefore also not experiencing any attenuation from the normalized radiation pattern.

The deployment tool will only place a drone if the possition is feasable meaning that if the user is inside a building which is higher then the fly height of the drone, no UABS would be place. In normal circumstances, with more UABSs, annother nearby drone would try to take over the responsibility. However, since only one drone is available in this scenario, the user would remain uncovered. To make sure only covered users are considered in this scenario, the user in question will always be located in the same outdoor location. The location chosen for this situation is longitude 3.73311°E and latitude 51.05992°N.

5.2.2 The influence from the maximum transmission power

LTE makes usages of power control meaning that no more power will be used then strictly necessary. The actual transmit power P_{tx} therefore ranges between 0 and the maximum input power. P_{tx} is zero when either no user is present or the user is so far away that the actual tranmit power would exceed the maximum transmission power.

Increasing the maximum tranmission power won't influence the power consumption or SAR_{10g} because the UABS won't use more then strictly required. It is therefore more usefull to match the transmission power against a variable fly height. Figure 5.6 shows a logarithmic relationship showing that P_{tx} increases fast at low altitude but slows down at lower altitudes.

Since it became clear from section 5.2.1 that the type of antenna won't make a difference when applying the tool in this scenario, it is not usefull to repeat this test with different types of

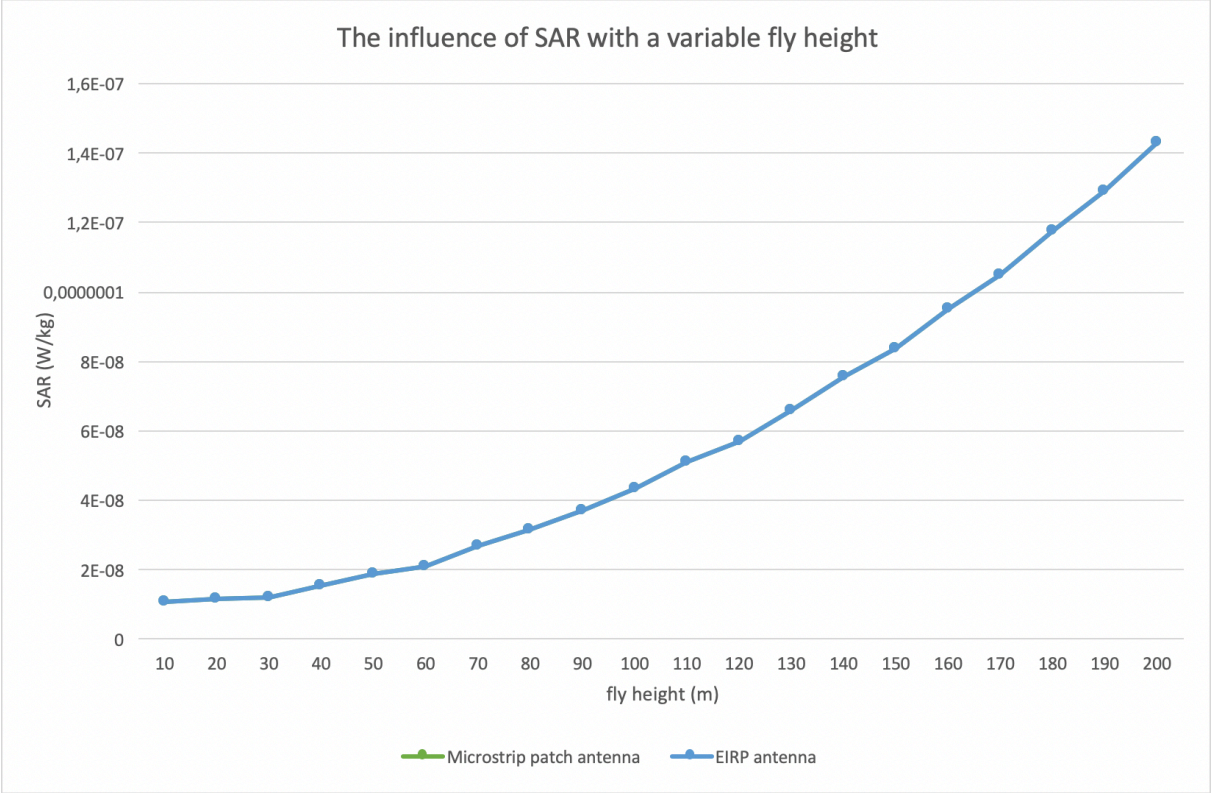

Figure 5.4: General design of a microstrip antenna

antennae.

5.3 Scenario 2: increased traffic

5.3.1 Influence of the flight altitude

The first case of this scenario investigates the influ

5.4 Scenario 3:

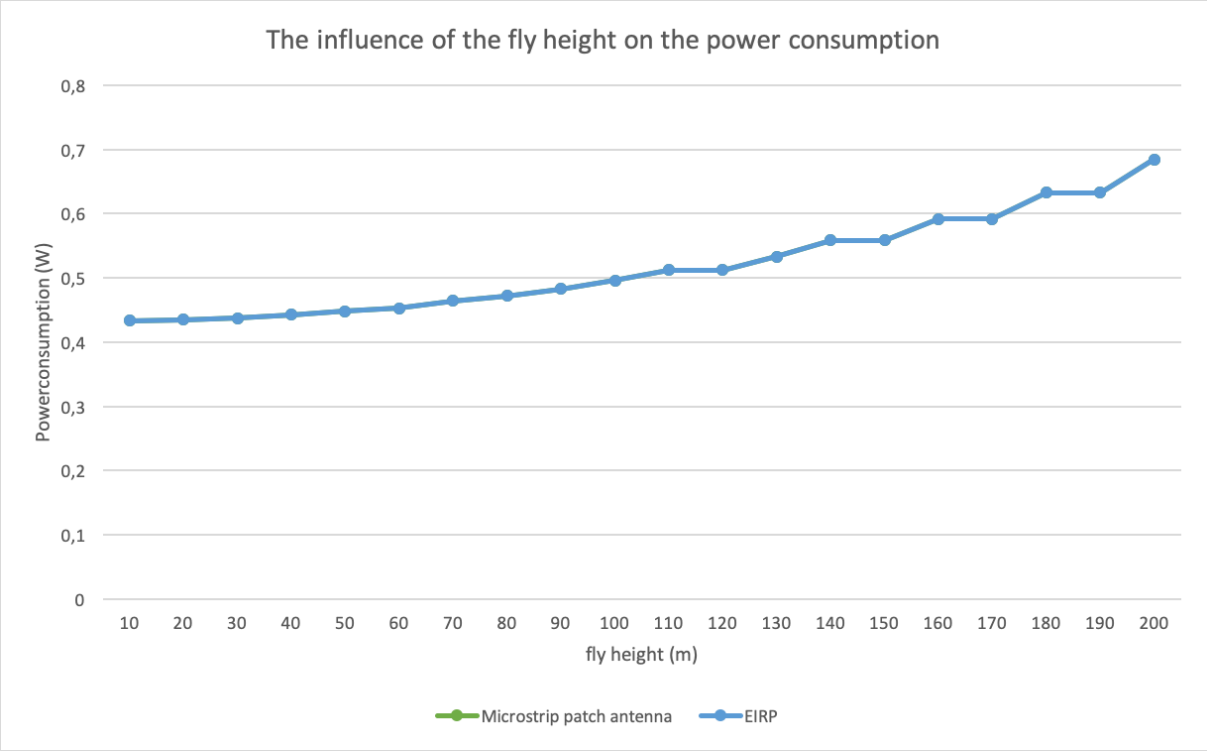

Figure 5.5: General design of a microstrip antenna

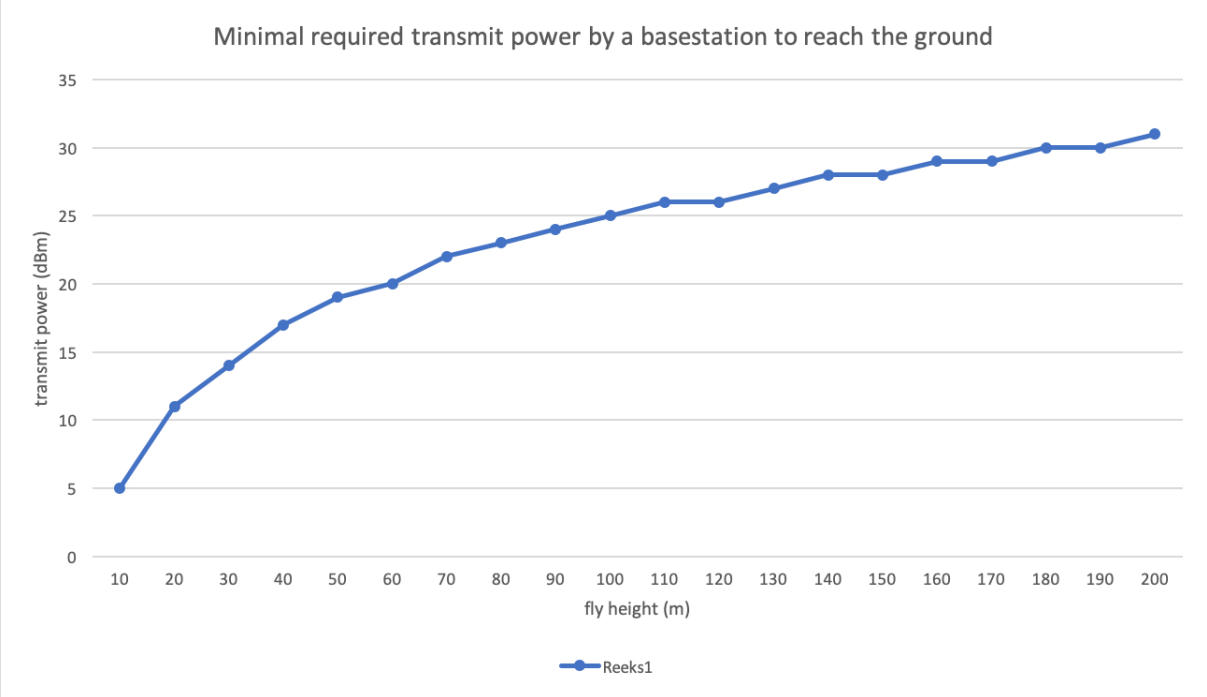

Figure 5.6: General design of a microstrip antenna

6

Conclusions

todo

Bibliography

[1] *5G Wireless Systems Simulation and Evaluation Techniques*. Springer.

[2] D. standaard, "Base overschreed stralingsnormen na aanslagen," *De standaard*, 2016.

[3] L. Hardell and C. Sage, "Biological effects from electromagnetic field exposure and public exposure standards," *Biomedicine and Pharmacotherapy*, vol. 62, no. 2, pp. 104 – 109, 2008.

[4] "Electromagnetic fields (emf)," Nov.

[5] M. Deruyck, J. Wyckmans, W. Joseph, and L. Martens, "Designing uav-aided emergency networks for large-scale disaster scenarios," *EURASIP Journal on Wireless Communications and Networking*, vol. 2018, 12 2018.

[6] v. v. d. v. e. l. Federale overheidsdienst: volksgezondheid, "Elektromagnetische velden en gezondheid: Uw wegwijzer in het elektromagnetische landschap," vol. 5, 2014.

[7] "Normen zendantennes." `https://omgeving.vlaanderen.be/normen-zendantennes`. Accessed: 14-10-2019.

[8] I. Guideline, "Guidelines for limiting exposure to time-varying electric, magnetic, and electromagnetic fields (up to 300 ghz)," *Health phys*, vol. 74, no. 4, pp. 494–522, 1998.

[9] D. Plets, W. Joseph, K. Vanhecke, and L. Martens, "Exposure optimization in indoor wireless networks by heuristic network planning," *Progress In Electromagnetics Research*, vol. 139, pp. 445–478, 01 2013.

[10] M. Deruyck, E. Tanghe, D. Plets, L. Martens, and W. Joseph, "Optimizing lte wireless access networks towards power consumption and electromagnetic exposure of human beings," *Computer Networks*, vol. 94, 12 2015.

[11] D. Plets, W. Joseph, S. Aerts, K. Vanhecke, G. Vermeeren, and L. Martens, "Prediction and comparison of downlink electric-field and uplink localised sar values for realistic indoor wireless planning," *Radiation Protection Dosimetry*, vol. 162, no. 4, pp. 487–498, 2014.

[12] D. Plets, W. Joseph, K. Vanhecke, and L. Martens, "Downlink electric-field and uplink sar prediction algorithm in indoor wireless network planner," in *The 8th European Conference on Antennas and Propagation (EuCAP 2014)*, pp. 2457–2461, IEEE, 2014.

[13] S. Kuehn, S. Pfeifer, B. Kochali, and N. Kuster, "Modelling of total exposure in hypothetical 5g mobile networks for varied topologies and user scenarios," *Final Report of Project CRR-816, Available on line at: https://tinyurl. com/r6z2gqn*, 2019.

[14] D. Plets, W. Joseph, K. Vanhecke, G. Vermeeren, J. Wiart, S. Aerts, N. Varsier, and L. Martens, "Joint minimization of uplink and downlink whole-body exposure dose in indoor wireless networks," *BioMed research international*, vol. 2015, 2015.

[15] I. Singh and V. Tripathi, "Micro strip patch antenna and its applications: a survey," *Int. J. Comp. Tech. Appl*, vol. 2, no. 5, pp. 1595–1599, 2011.

[16] K. Kashwan, V. Rajeshkumar, T. Gunasekaran, and K. S. Kumar, "Design and characterization of pin fed microstrip patch antennae," in *2011 Eighth International Conference on Fuzzy Systems and Knowledge Discovery (FSKD)*, vol. 4, pp. 2258–2262, IEEE, 2011.

[17] A. Sudarsan and A. Prabhu, "Design and development of microstrip patch antenna," *International Journal of Antennas (JANT) Vol*, vol. 3, 2017.

[18] "Bundesamt für strahlenschutz." `http://www.bfs.de/SiteGlobals/Forms/Suche/BfS/EN/SARsuche_Formular.html`. Accessed: 14-10-2019.

[19] P. Joshi, D. Colombi, B. Thors, L.-E. Larsson, and C. Törnevik, "Output power levels of 4g user equipment and implications on realistic rf emf exposure assessments," *IEEE Access*, vol. 5, pp. 4545–4550, 2017.

[20] I. Singh and V. Tripathi, "Micro strip patch antenna and its applications: a survey," *Int. J. Comp. Tech. Appl*, vol. 2, no. 5, pp. 1595–1599, 2011.

Appendices

A

Radiation patterns: datasheet

Table A.1 gives an overview of the attenuation in the E and H plane. The first radiation pattern is with a square groundplane with an edge of 0.060 meter while the second pattern is more of a rectangular shape with a width of 0.0524m and a lenght of 0.0438m. All other settings are equal as defined in 4.2.4

Table A.1: Overview of attenuation in dBm

	pattern 1		pattern 2	
angle	E	H	E	H
0	0,00	0,00	0	0
10	-0,17	-0,14	-0.1561	-0.158
20	-0,67	-0,57	-0.5797	-0.6257
30	-1,48	-1,27	-1.263	-1.386
40	-2,57	-2,22	-2.193	-2.412
50	-3,90	-3,39	-3.357	-3.665
60	-5,40	-4,73	-4.741	-5.099
70	-7,09	-6,23	-6.337	-6.658
80	-8,82	-7,87	-8.136	-8.278
90	-10,54	-9,70	-10.11	-9.88
100	-12,20	-11,84	-12.14	-11.34
110	-13,73	-14,37	-13.81	-12.47
120	-15,04	-17,65	-14.42	-13.00
130	-16,01	-21,83	-13.72	-12.82
140	-16,47	-23,63	-12.41	-12.08
150	-16,42	-20,37	-11.15	-11.15
160	-16,05	-17,49	-10.21	-10.33
170	-15,69	-15,93	-9.683	-9.786
180	-15,54	-15,54	-9.596	-9.596
190	-15,69	-16,30	-9.963	-9.784
200	-16,05	-18,44	-10.79	-10.33
210	-16,42	-22,85	-12.07	-11.15
220	-16,47	-31,23	-13.71	-12.07
230	-16,00	-24,07	-15.25	-12.80
240	-15,03	-18,05	-15.65	-12.99
250	-13,72	-14,42	-14.3	-12.45
260	-12,20	-11,81	-12.11	-11.33
270	-10,54	-9,70	-9.882	-9.866
280	-8,82	-7,87	-7.859	-8.267
290	-7,09	-6,23	-6.069	-6.649
300	-5,40	-4,73	-4.502	-5.093
310	-3,90	-3,39	-3.154	-3.661
320	-2,57	-2,22	-2.029	-2.409
330	-1,48	-1,27	-1.138	-1.384
340	-0,67	-0,57	-0.4963	-0.6246
350	-0,17	-0,14	-1143	-0.1575

B

Radiation patterns: example configuration

In listing 2 is an possible configuration described for a radiation pattern. It is important to notice that this example configuration does not represent the used configuration in this master dissertation. The `radiatoinPattern`-tag consist of a `slices`-tag. This tag can contain as mutch slices as desired. In this example, 3 slices are defined indicated with the `attenautaion`-tag. An attenuation-tag contaisn a mandatory attribute `az` which defines the azimuth angle to which all underlying attenuation values belong. Inside the `attenuation` tag are all attenuation values written in a `value`-tag.

The tool distributes all values equally over 180°. In the example below, each `attenuation` tag contains 10 values meaning there the exact attenuation is known every 20°.

The highlighted value of -14,42 is therefore measured at an azimuth angle of 0° and an elevation angle of 120° (counterclockwise).

```
<radiationPattern>
    <slices>
        <attenuation az="0">
            <value>0</value>
            <value>-0.5797</value>
            <value>-2.193</value>
            <value>-4.741</value>
            <value>-8.136</value>
            <value>-12.14</value>
            <value>-14.42</value>
            <value>-12.41</value>
            <value>-10.21</value>
            <value>-9.596</value>
        </attenuation>
        <attenuation az="180">
            <value>0</value>
            <value>-0.4963</value>
            <value>-2.029</value>
            <value>-4.502</value>
            <value>-7.859</value>
            <value>-12.11</value>
            <value>-15.65</value>
            <value>-13.71</value>
            <value>-10.79</value>
            <value>-9.596</value>
        </attenuation>
        <attenuation az="90">
            <value>0</value>
            <value>-0.6257</value>
            <value>-2.412</value>
            <value>-5.099</value>
            <value>-8.278</value>
            <value>-11.34</value>
            <value>-13.00</value>
            <value>-12.08</value>
            <value>-10.33</value>
            <value>-9.596</value>
        </attenuation>
    </slices>
</radiationPattern>
```

Listing 2: Example configuraton of a radiation pattern.